Proceedings of the ASME 2020
Dynamic Systems and Control Conference
DSCC 2020
October 4-7, 2020, Pittsburgh, USA

DSCC2020-3180

COMBINING NON-PARAMETRIC AND PARAMETRIC MODELS FOR STABLE AND COMPUTATIONALLY EFFICIENT BATTERY HEALTH ESTIMATION

Antti Aitio
Battery Intelligence Lab
Department of Engineering Science
University of Oxford
OX1 3PJ, Oxford, UK
Email: antti.aitio@eng.ox.ac.uk

David Howey
Battery Intelligence Lab
Department of Engineering Science
University of Oxford
OX1 3PJ, Oxford, UK
Email: david.howey@eng.ox.ac.uk

ABSTRACT

Equivalent circuit models for batteries are commonly used in electric vehicle battery management systems to estimate state of charge and other important latent variables. They are computationally inexpensive, but suffer from a loss of accuracy over the full range of conditions that may be experienced in real-life. One reason for this is that the model parameters, such as internal resistance, change over the lifetime of the battery due to degradation. However, estimating long term changes is challenging, because parameters also change with state of charge and other variables. To address this, we modelled the internal resistance parameter as a function of state of charge and degradation using a Gaussian process (GP). This was performed computationally efficiently using an algorithm [1] that interprets a GP to be the solution of a linear time-invariant stochastic differential equation. As a result, inference of the posterior distribution of the GP scales as $\mathcal{O}(n)$ and can be implemented recursively using a Kalman filter.

INTRODUCTION

Battery management systems in electric vehicles often employ electrical equivalent circuit models (ECMs) to control battery packs. These models commonly include an open circuit voltage source, one or more RC pairs and a series resistance. In comparison to 'physics-based' battery models such as the so-called Doyle-Fuller-Newman model [2,3], or reduced-order models derived from it [4], equivalent circuits have much lower computational cost. However, with simplicity comes limited performance over the range of states of charge and temperatures experienced in EV use, and this is partly due to parameter variations [5,6]. In addition, during operation, accuracy typically deteriorates as batteries age. Due to the complexity of degradation [7], modelling the dependency of battery model parameters on aging remains a challenge.

To improve the performance of ECMs, model parameters may be considered functions of state of charge (SoC), temperature and other variables, such as battery age or other stress factors influencing state of health. For this study, the series resistance of a simple first-order electrical equivalent circuit is modelled as a function of state of charge and degradation using a Gaussian process (GP), a type of non-parametric model. ('Non-parametric' models can be thought of as having infinite dimensional parameters, i.e. their 'parameters' are actually functions. In this paper we also refer to non-parametric models as 'functional parameters'.) First, a ground-truth is established by simulating the battery voltage response to an electric vehicle load calculated from the urban dynamometer driving schedule (UDDS) using a first-order RC-circuit, with the series resistance being a given function of SoC and degradation. This function is then retrieved back from the data as the posterior distribution of a Gaussian process. Inference is conducted using the linear time-invariant stochastic differential equation framework [1, 8] of Gaussian processes, allowing for computationally efficient recursive methods to be

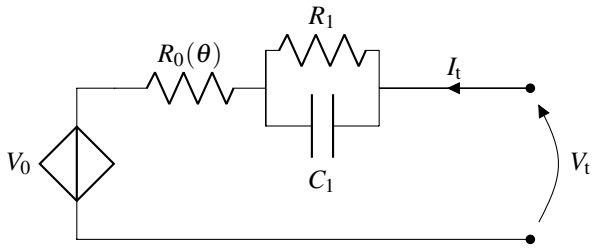

FIGURE 1. First order RC circuit. The series element resistor R_0 is considered a function of both SoC and degradation.

used. The resulting estimation is implemented as a modified extended Kalman filter, enabling stable joint estimation of battery states and the functional parameter at the same time.

Previous work on joint online estimation of battery states and parameters has focused on Bayesian filtering techniques [9–12] and adaptive observers [13, 14]. However, rudimentary or no parameter dynamics were assumed, which in the latter case results in random walk parameter evolution and no ability to forecast future behaviour accurately. Furthermore, when using explicit dynamics, such as in [14], their functional form has to be *a priori* determined, which for battery degradation remains a significant challenge. In contrast, our key contribution in this paper is to incorporate the learning of parameter dynamics within a flexible and computationally efficient approach that extends joint Bayesian filtering techniques for combined SoC/SoH estimation.

EXTENDED EQUIVALENT CIRCUIT MODEL

The proposed ECM is illustrated in Fig. 1. The circuit consists of an open circuit voltage source V_0, a single RC-pair, and a series resistance dependent on parameters θ, representing SoC and degradation. The continuous-time system dynamics are

$$\dot{x} = \frac{I_t}{Q} \tag{1a}$$

$$\dot{V}_{RC} = -\frac{V_{RC}}{R_1 C_1} + \frac{I_t}{C_1} \tag{1b}$$

$$V_t = V_0(x) + V_{RC} + R_0(\theta) I_t, \tag{1c}$$

where x is the state of charge, V_{RC} the voltage across the RC pair, V_0 the open circuit voltage, V_t the measured terminal voltage and I_t the input current (positive on charging). There are two dynamic states, namely x and V_{RC}. It is assumed that the OCV function, $V_0(x)$, and parameters, R_1 and C_1, are known. The functional parameter $R_0(\theta)$ is jointly estimated with the battery states.

In practical applications, the function describing the dependency of the series resistance R_0 on SoC is not well known and is experimentally fitted [15, 16]. Various physics-based [17] and semi-empirical models [18] for Li-ion battery degradation illustrate that the direct mapping of model parameters to 'stress factors' impacting degradation is difficult to establish. Modelling the function R_0 as a Gaussian process provides a flexible approach for estimation, which may be performed online using a recursive algorithm as described below.

GAUSSIAN PROCESS REGRESSION

A Gaussian process is a collection of random variables, any subset of which has a joint Gaussian distribution. This defines a prior distribution over functions, which can be used to yield a posterior when conditioned with observed data. By definition, GPs may be represented by a mean and covariance of a multivariate Gaussian, that is,

$$\begin{aligned} f(x) &\sim GP(\mu(x), k(x,x')) \text{ , where} \\ \mu(x) &= \mathbb{E}[f(x)], \\ k(x,x') &= \mathbb{E}\left[(f(x)-\mu(x))(f(x')-\mu(x'))\right]. \end{aligned} \tag{2}$$

Without loss of generality, it may be assumed that the Gaussian process has zero mean, so that $\mu(x) = 0$. Therefore the Gaussian process may be entirely described by its covariance function $k(x,x')$. There exist many different covariance functions for GPs [19]. The Matérn family of functions,

$$k(x,x') = \sigma^2 \frac{2^{1-\nu}}{\Gamma(\nu)} \left(\sqrt{2\nu}\frac{|x-x'|}{l}\right)^{\nu} K_\nu \left(\sqrt{2\nu}\frac{|x-x'|}{l}\right), \tag{3}$$

are used in many applications. Here K_ν is the Bessel function of the second kind and σ, ν and l are the hyperparameters. The parameter ν is often poorly identifiable from data and is chosen *a priori* [20]. A very commonly used covariance function, the squared exponential (SE), is obtained as $\nu \to \infty$ [19],

$$k(x,x') = \sigma^2 \exp\left(-\frac{|x-x'|^2}{2l^2}\right). \tag{4}$$

Fig. 2 illustrates the effect of varying ν on the smoothness of the GP. Covariance functions in the Matérn family are stationary and isotropic, depending only on the Euclidean distance between inputs, $|x-x'|$, making them translation-invariant. The parameters σ and l control the magnitude and length scale of the Gaussian process and may be inferred by maximising the marginal likelihood of observing the data (in the absence of measurement noise) [19], conditional on $\theta_h \in [\sigma, l]$,

$$\log p(y|X,\theta_h) = -y^T k(\theta_h, X)^{-1} y - \frac{1}{2}\log|k(\theta_h, X)| - \frac{n}{2}\log 2\pi, \tag{5}$$

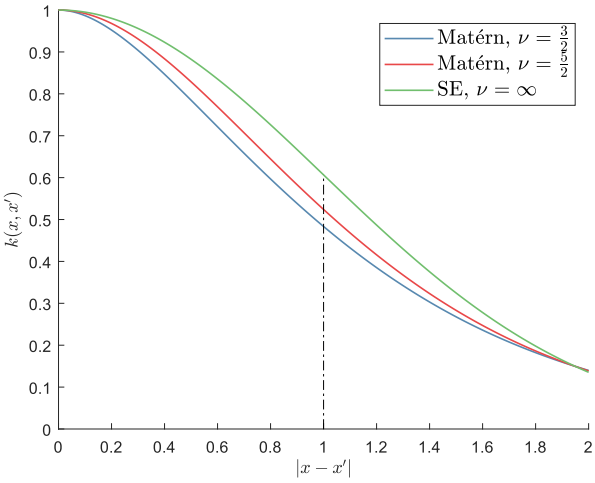

FIGURE 2. COMPARISON OF MATÉRN FAMILY OF COVARIANCE FUNCTIONS WITH $\sigma^2 = 1$, $l = 1$.

where n is the input dimension, y are the observations, and $|\cdot|$ represents the determinant. For notational convenience, $k(\theta_{\mathrm{h}}, X)$ represents the covariance function parameterised with θ_h and input X. Given the covariance function and its hyperparameters, the task in Gaussian process regression consists of finding the posterior distribution of the function given the input-output training data (X, y) and mean and covariance functions. Prediction using the model may then be performed by integrating over the posterior distribution given the new inputs. As the posterior distribution $p(f|X,y)$ is Gaussian, the predictive distribution has a closed form solution that is derived from the joint distribution of training and test points [21],

$$\begin{aligned} p(f_*|X_*,X,f) &= N(f_*|\mu_*,\Sigma_*) \\ \mu_* &= \mu(X_*) + k(X,X_*)^T k(X,X)^{-1}(f-\mu(X)) \\ \Sigma_* &= k(X_*,X_*) - k(X,X_*)^T k(X,X)^{-1} k(X,X_*), \end{aligned} \tag{6}$$

where X_*, f_* denotes the test input points and predictions and X, f the corresponding training points.

GP representation as linear dynamic system

Both the calculation of the marginal likelihood (5) and the predictive distribution (6) require the inversion of the covariance matrix $k(X,X')$. Since $k \in \mathbb{R}^{nxn}$, where n is the dimension of input x, and the computation of the inverse of k scales as $\mathcal{O}(n^3)$, a batch approximation quickly becomes unfeasible as n grows. Many sparse approximation techniques exist to reduce the computational load of inference [22,23]. One such technique, achieving $\mathcal{O}(n)$ in computational effort, is to consider the Gaussian process to be a solution to a linear time-invariant stochastic partial differential equation [1, 8, 20],

$$\frac{\partial f(x,t)}{\partial t} = Ff(x,t) + Lw(x,t), \tag{7}$$

where F is the transition matrix, L the dispersion matrix and $w(x,t)$ the noise process. This spatio-temporal model has been used in applications such as geostatistical modelling [1,24]. The approach uses the Fourier-domain representation of the covariance function, which, by the Wiener-Khinchine theorem, represents the spectral density of the underlying stationary stochastic process. As shown by [1, 25], the spectral density in temporal and spatial Fourier dimensions $(\omega_{\mathrm{x}}, \omega_{\mathrm{t}})$ may be factorized to be of the form

$$S(\omega_x, \omega_t) = G(i\omega_x, i\omega_t) q(\omega_x) G(-i\omega_x, -i\omega_t), \tag{8}$$

where $G(i\omega_x, i\omega_t)$ is a stable transfer function and $q(\omega_x)$ the spectral density of the white noise driving the stochastic process. Provided G is strictly proper, a corresponding state-space realization is easily retrieved.

FUNCTIONAL PARAMETER AS A TWO-DIMENSIONAL GAUSSIAN PROCESS

In order to enable the series resistance R_0 in the equivalent circuit (1) to be a function of both SoC and degradation, it is modeled as a zero-mean Gaussian process with covariance function given by

$$k(x,t) = \sigma^2 \exp\left(-a_{\mathrm{x}}|x|^2\right) \exp\left(-a_{\mathrm{t}}|t|^2\right), \tag{9}$$

where $a_{\mathrm{x,t}} = (2l_{\mathrm{x,t}}^2)^{-1}$. The use of the product of covariance functions makes $k(x,t)$ separable in both time and frequency domains and allows for separate length scales to be used. The SE is chosen due to its smoothness over other Matérn functions in the normalised interval $|x| \leq 1$ (see Fig. 2). For the purposes of estimating R_0, we treat SoC as the 'spatial' domain, x, and degradation as the 'temporal' domain, t, to produce a linear system of the type in (7). Following the procedure outlined in [25], taking the Fourier transform of this covariance function gives the spectral representation,

$$\begin{aligned} &S(\omega_{\mathrm{x}}, \omega_{\mathrm{t}}) = \\ &\sigma^2 \left(\frac{\pi}{a_{\mathrm{x}}}\right)^{\frac{1}{2}} \exp\left(-\frac{\omega_{\mathrm{x}}^2}{4a_{\mathrm{x}}}\right) \left(\frac{\pi}{a_{\mathrm{t}}}\right)^{\frac{1}{2}} \exp\left(-\frac{\omega_{\mathrm{t}}^2}{4a_{\mathrm{t}}}\right). \end{aligned} \tag{10}$$

Since this is separable in x and t, it may be factorized as

$$S(\omega_{\mathrm{x}}, \omega_{\mathrm{t}}) = G(i\omega_{\mathrm{t}}) q(\omega_{\mathrm{x}}) G(-i\omega_{\mathrm{t}}). \tag{11}$$

As the transfer function $G(i\omega_t)$ is not rational, a 4th order Taylor expansion is taken as an approximation [8]. This gives a linear dynamic system of the form (7), where

$$F_0 = \begin{bmatrix} 0 & 1 & 0 & 0 \\ 0 & 0 & 1 & 0 \\ 0 & 0 & 0 & 1 \\ -a_0 & -a_1 & -a_2 & -a_3 \end{bmatrix}, \; x_0 = \begin{bmatrix} f(x,t) \\ \frac{\partial f(x,t)}{\partial t} \\ \frac{\partial^2 f(x,t)}{\partial t^2} \\ \frac{\partial^3 f(x,t)}{\partial t^3} \end{bmatrix} L_0 = \begin{bmatrix} 0 \\ 0 \\ 0 \\ 1 \end{bmatrix}, \quad (12)$$

with a_n representing the coefficients in the denominator of G. The spatially resolved white noise $w(x,t)$ has a spectral density q given by [8, 25]

$$q = k(x) \otimes \underbrace{\sigma^2 N! \sqrt{\frac{\pi}{a_t}} (4a_t)^N}_{\text{temporal spectral density}}, \quad (13)$$

where the temporal spectral density is due to the Taylor approximation of $G(i\omega_t)$ where $N = 4$ and

$$k(x) = \exp(-a_x |x|^2), \quad (14)$$

which is retrieved from the inverse Fourier transform of $q(\omega_x)$ and is simply the spatial part of (9). The representation (12)-(14) remains infinite-dimensional in SoC terms, x. To obtain a finite dimensional representation, the x-domain is represented by 10 equispaced triangular basis functions, which results in a block-diagonal representation where $F = I(10) \otimes F_0$, $L = I(10) \otimes L_0$, $x = \mathbf{1} \otimes x_0$, $\mathbf{1}$ representing a vector of ones and $I(10)$ the identity of size 10. The spatial covariance function, $k : \mathbb{R}^{10} \mapsto \mathbb{R}^{10x10}$, is evaluated at basis function centres.

Recursive inference of GP using the Kalman filter

Recursive inference of a Gaussian process in the form of linear time-invariant system (12), (14) may be done using the Kalman filter framework. The initial covariance $P_{GP,0}$ should be defined carefully in order to describe a GP. It may be obtained from the solution to the matrix Lyupanov equation [8],

$$\frac{dP}{dt} = FP + PF^T + LqL^T = 0. \quad (15)$$

The discrete-time process noise covariance, Q_{GP}, for the GP may be efficiently calculated [26] from $P_{GP,0}$ as

$$Q_{GP} = P_{GP,0} - AP_{GP,0}A^T, \quad (16)$$

where A is the matrix exponential $\text{expm}(Ft_s^*)$, with t_s^* being the sampling step size. Here the temporal dimension is degradation, where the metric used is the charge throughput during the ageing of the battery, making the sampling step

$$t_s^* = \int_{t_0}^{t} |I| \, dt \quad (17)$$

in the time interval [t_0,t].

Joint estimation of GP and battery states

The Kalman filter inference framework may be extended by incorporating the battery state estimation task resulting from the equivalent circuit model (1). The resulting system jointly estimates SoC, the overpotential V_{RC} and the series resistance (as a GP), recursively. The resulting system dynamics are block diagonal with respect to the battery states and the Gaussian process, which in discrete time is represented by

$$\begin{bmatrix} z_{Batt} \\ z_{GP} \end{bmatrix}_{t+1} = \underbrace{\begin{bmatrix} A_{Batt} & 0 \\ 0 & \text{expm}(Ft_s^*) \end{bmatrix}}_{A_{sys}} \begin{bmatrix} z_{Batt} \\ z_{GP} \end{bmatrix}_t + BI_t + \varepsilon, \quad (18)$$

where

$$z_{Batt} \in [x, V_{RC}]^T, \; z_{GP} \in \mathbb{R}^{40}, \; \varepsilon \sim N(0, Q_{sys}),$$

z_{GP} being the set of states due to the GP. The continuous time transition matrix for the Gaussian Process is F, and

$$A_{Batt} = \begin{bmatrix} 1 & 0 \\ 0 & \exp(-\frac{t_s}{R_1 C_1}) \end{bmatrix}, B = \begin{bmatrix} t_s/Q \\ R_1 \left(1 - \exp(-\frac{t_s}{R_1 C_1})\right) \\ 0 \\ \vdots \end{bmatrix}, \quad (19)$$

where t_s is the sampling step size. Similarly, the process noise covariance matrix may be defined as a block diagonal,

$$Q_{sys} = \begin{bmatrix} Q_x & 0 & 0 \\ 0 & Q_{V_{RC}} & 0 \\ 0 & 0 & Q_{GP} \end{bmatrix}. \quad (20)$$

The system is linear apart from $V_0(x)$, modeled by a polynomial which is a cubic approximation of the OCV calculated by [27] for a Li-NMC cell at 25 °C,

$$V_0(x) = 3.64 + 0.55x - 0.72x^2 + 0.75x^3. \quad (21)$$

Initialization:

$z^+_{\text{Batt,t}} = z^+_{\text{Batt,0}}$

$z^+_{\text{GP,t}} = 0$

$P^+_{Batt,t} = 0.0001I$

$P^+_{\text{GP,t}} = P_{\text{GP,0}}$

$Z^+_{\text{t}} = [z^+_{\text{Batt,t}}\ z^+_{\text{GP,t}}]^T$

$P^+_{\text{t}} = \text{blkdiag}(P^+_{Batt,t}\ ,\ P^+_{\text{GP,t}})$

$\Phi = -\log p(\theta)$

Propagation:

$Z^-_{\text{t}} = A_{\text{sys}} Z^+_{\text{t-1}} + BI_{\text{t-1}}$

$P^-_{\text{t}} = A_{\text{sys}} P^+_{\text{t-1}} A^T_{\text{sys}} + Q_{\text{sys}}$

Measurement and update:

$\hat{V}_{\text{t}} = h(Z^-_{\text{t}}, I_{\text{t}})\ ,\ e_t = (V_{\text{t}} - \hat{V}_{\text{t}})$

$S_{\text{t}} = H_{\text{t}} P^-_{\text{t}} H^T_{\text{t}} + R$

$K_{\text{t}} = P^-_{\text{t}} H^T_{\text{t}} S^{-1}_{\text{t}}$

$Z^+_{\text{t}} = Z^-_{\text{t}} + K_{\text{t}} e_{\text{t}}$

$P^+_{\text{t}} = P^-_{\text{t}} - K_{\text{t}} S_{\text{t}} K^T_{\text{t}}$

Energy function update:

$\Phi = \Phi + \frac{1}{2}\log(|2\pi S_{\text{t}}|) + \frac{1}{2} e^T_{\text{t}} S^{-1}_{\text{t}} e_{\text{t}}$

TABLE 1. EXTENDED JOINT KALMAN FILTER RECURSION USING SYSTEM (18)-(22). H_{t} IS THE JACOBIAN OF THE MEASUREMENT EQUATION $h(Z^-_t, I_t)$ CALCULATED AT EACH TIMESTEP.

Due to this non-linearity, the extended Kalman filter (or similar) is required for estimation. The measurement equation for the system is

$$h(x_{\text{t}}, V_{\text{RC,t}}, z_{\text{GP,t}}, I_{\text{t}}) = V_0(x_{\text{t}}) + V_{\text{RC,t}} + \Psi(x_{\text{t}}) D_{\text{GP}} z_{\text{GP,t}} I_{\text{t}}, \quad (22)$$

where $\Psi(x)$ is the vector of triangular basis functions to project the reduced-dimensional representation of the Gaussian Process to the current SoC value and $D_{\text{GP}} = I(10) \otimes [1\ 0\ 0\ 0]$ is a sparse matrix such that the 1 appears for the first term in the Gaussian process dynamics at each spatial location and represents the value of the series resistance $R_0(x, t^*)$. The joint extended Kalman filter recursion is shown in Table 1.

Hyperparameter estimation using the EKF recursion

In addition to approximating the posterior distribution of the functional parameter R_0, the Kalman filter recursion also provides the calculation required for the Bayesian inference of the hyperparameter vector $\theta_{\text{h}} \in [l_{\text{x}}, l_{\text{t}}]$. By Bayes' rule, the posterior parameter distribution is given by

$$p(\theta_{\text{h}}|y) = \frac{p(y|\theta_{\text{h}}) p(\theta_{\text{h}})}{p(y)}, \quad (23)$$

where $p(y|\theta_{\text{h}})$ is the likelihood of observing the data given θ_{h} and $p(\theta_{\text{h}})$ the prior distribution of θ_{h}. To approximate the posterior distribution $p(\theta_{\text{h}}|y)$, various methods such as Markov Chain Monte Carlo (MCMC) [28] or variational inference [29] may be used. For the purposes of estimating the hyperparameters in this study, a uniform prior is assumed for them. The Kalman filter provides a method of recursively estimating the so-called energy function (Table 1), that is the negative unnormalized logarithm of the posterior parameter probability,

$$\Phi = -\log p(\theta|y) = -\log p(y|\theta) - \log p(\theta). \quad (24)$$

With a uniform prior, the second term in (24) is constant, meaning the maximum likelihood estimate (MLE) of the hyperparameters is therefore achieved by minimising Φ. A Gaussian approximation of the posterior is made by using Laplace's approximation [21] around the MLE point (the mode of the posterior) to estimate the variance, giving

$$p(\theta|y) \sim N(\theta_{\text{ML}}, \hat{\Sigma})\ \ \text{,where}\ \ \hat{\Sigma} = \left.\frac{\partial^2 \phi}{\partial \theta^2}\right|^{-1}_{\theta_{\text{ML}}}. \quad (25)$$

Smoothed estimates

The forward posterior distribution of the system obtained from the EKF recursion includes information up to the point of measurement, expressing the probability $p(Z_{\text{t}}|y_{1:\text{t}})$. To retrieve smoothed estimates of $R_0(x, t^*)$, the probability distribution can be conditioned on all the measurements in the data, that is $p(Z_{\text{t}}|y_{1:\text{T}})$, where T represents the last time index. The smoothed mean and covariance are obtained through the Rauch-Tung-Striebel smoother (RTSS) [30]. The algorithm consists of a backward pass through the data having first obtained a history of the prior and posterior mean and covariance estimates for each point in time (Table 2). The RTSS is key to the estimation of the functional parameter using a Gaussian process with noisy data. Specifically, using the smoothed estimate as a starting point, both interpolation and to some degree, extrapolation, may be performed.

SIMULATIONS

Generating synthetic ground-truth data

To produce a ground-truth dataset, a Li-ion cell was simulated using a fully known system (1) with the series resistance

Initialization:

$\mu_{\mathrm{T}}^{\mathrm{s}} = \mu_{\mathrm{T}}^{+}$

$P_{\mathrm{T}}^{\mathrm{s}} = P_{\mathrm{T}}^{+}$

Backward recursion:

$\mu_{\mathrm{t+1}}^{-} = A_{\mathrm{t}}\mu_{\mathrm{t}}$

$P_{\mathrm{t+1}}^{-} = A_{\mathrm{t}}P_{\mathrm{t}}A_{\mathrm{t}}^{T} + Q_{\mathrm{t}}$

$G_{\mathrm{t}} = P_{\mathrm{t}}^{+}A_{\mathrm{t}}^{T}(P_{\mathrm{t+1}}^{-})^{-1}$

$\mu_{\mathrm{t}}^{\mathrm{s}} = \mu_{\mathrm{t}}^{+} + G_t(\mu_{\mathrm{t+1}}^{\mathrm{s}} - \mu_{\mathrm{t+1}}^{-})$

$P_{\mathrm{t}}^{\mathrm{s}} = P_{\mathrm{t}}^{+} + G_{\mathrm{t}}\left(P_{\mathrm{t+1}}^{\mathrm{s}} - P_{\mathrm{t+1}}^{-}\right)G_{\mathrm{t}}^{T}$

TABLE 2. RAUCH-TUNG-STRIEBEL SMOOTHER ALGORITHM AS REPORTED BY [31]. THE PRIOR AND POSTERIOR MEAN AND COVARIANCE ESTIMATES ARE OBTAINED FROM THE FORWARD PASS OF THE KALMAN FILTER SHOWN IN TABLE 1.

function

$$R_0(x,t^*) = (0.005 + 0.004x^2 - 0.006x + \frac{0.0015}{1+e^{-6(t^*-1)}})\ \Omega, \quad (26)$$

with the x (SoC) dependency being similar in magnitude and shape to experimental results [16], and the t^* dependency being arbitrary. The parameters for the RC pair were set to $R_1 = 0.002\,\Omega$ and $C_1 = 8000\,\mathrm{F}$. The simulation consisted of 52 repetitions of the UDDS drive cycle sampled at 1Hz with load calculated by the `simVehicle` tool [32]. The drive cycle, simulated voltage response and SoC evolution over 1 cycle are shown in Fig. 3. The battery was 'recharged' every fourth cycle to bring it back to the initial SoC of 75%, giving an overall SoC range of 35%-75%. Upon recharge, the cycle was started with zero overpotential V_{RC}. The t^* input was calculated as the normalised total charge throughput, a proxy for battery ageing, having the range [0,1]. Gaussian white noise $e_t \sim N(0, 0.005^2)$ was added to the voltage response and was assumed fully known.

Results and discussion

The EKF algorithm with the coupled dynamic model (18)-(22), as described in Table 1, was used to estimate the posterior distribution of the function $R_0(x,t^*)$. The process noise variance elements $Q_x, Q_{V_{\mathrm{RC}}}$ were both set to 10^{-6}.

A uniform prior was used for the hyperparameters, making the minimisation of the energy function equivalent to the maximum likelihood estimate of the hyperparameters. Hyperparameter σ^2 was fixed at 10^{-4} and the two length scales l_{x}, l_{t^*} were

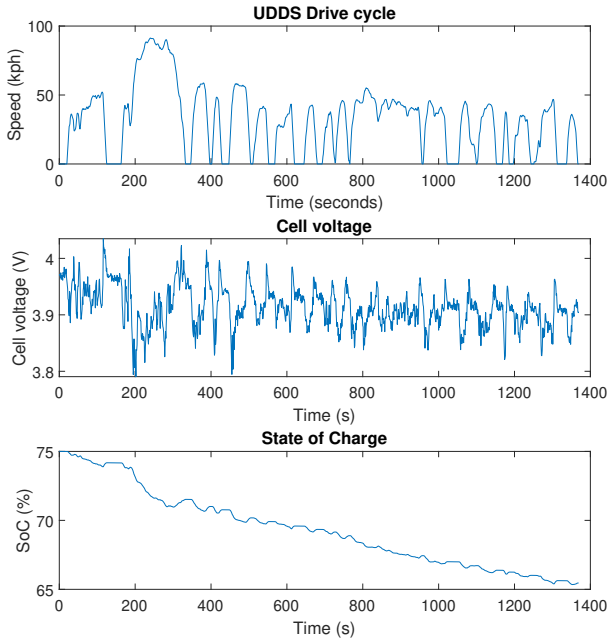

FIGURE 3. THE UDDS DRIVE CYCLE AND CALCULATED CELL VOLTAGE RESPONSE. THE CYCLE WAS REPEATED 52 TIMES WITH A RECHARGE EVERY FOURTH CYCLE.

Parameter	MLE	Estimated variance
l_{x}	1.768	0.1229
l_{t^*}	2.166	0.1002

TABLE 3. ESTIMATES FOR GP HYPERPARAMETERS

found using the `fmincon` function in MATLAB with lower and upper bounds for parameters set as 0 and 10 respectively. Following that, the variance of the parameters was calculated using Laplace's approximation at the MLE point by inverting the numerically calculated Hessian [33] of the energy function. The calculated values are shown in Table 3.

The smoothed distribution of $R_0(x,t^*)$ was calculated using the RTSS algorithm in Table 2. To ensure numerical stability, Tikhonov regularization with $\lambda = 10^{-12}$ was applied to the prior covariance matrix in the backward recursion, so that

$$G_{\mathrm{t}} = P_{\mathrm{t}}^{+}A_{\mathrm{t}}^{T}(P_{\mathrm{t+1}}^{-} + \lambda I)^{-1}. \quad (27)$$

The mean of the smoothed distribution is illustrated in Fig. 4, which also shows two cross-sections, one along the t^* dimension and another along the x dimension, together with confidence

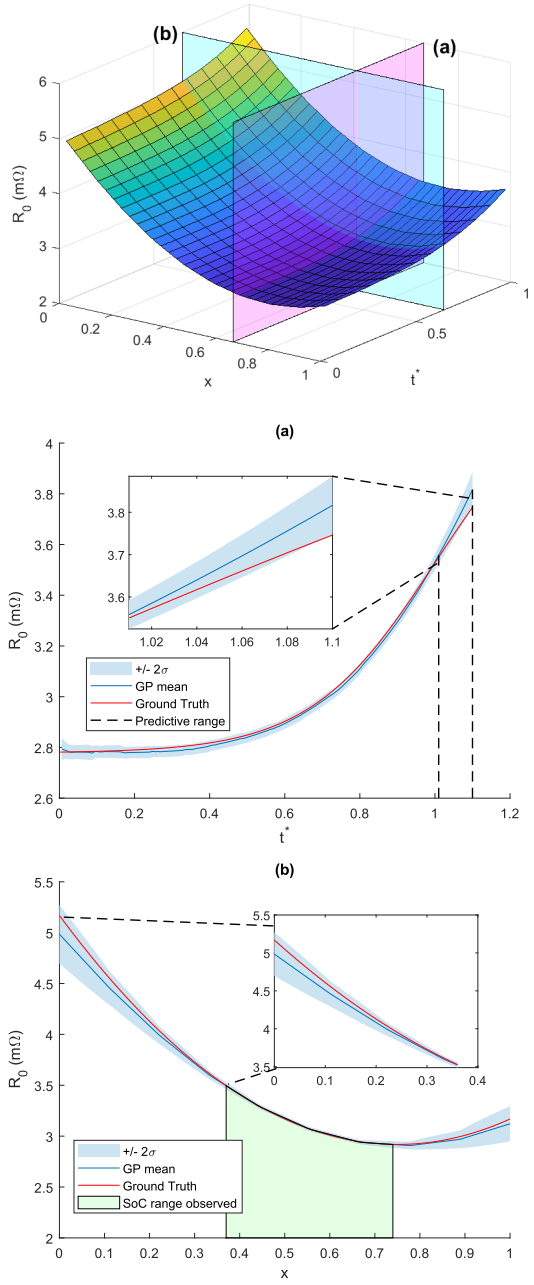

FIGURE 4. THE RTSS MEAN OF $R_0(x,t^*)$ OVER x AND t^*. SLICES (a) AND (b) HIGHLIGHTED WITH CONFIDENCE BOUNDS FROM THE MARGINAL DISTRIBUTION OF $R_0(x,t^*)$.

bounds calculated as the +/- 2σ values of the marginal smoothed distribution for R_0. The ground-truth is included in each case to illustrate the goodness of fit. The UDDS cycle gave an excursion in SoC of 35%-75%, therefore not covering the whole range of SoC. However, the method in this case extrapolates relatively well across the whole range even with the narrow portion observed. In the case of temporal variation at a single SoC location, slice (a), there is slight divergence at $0.2 < t^* < 0.5$. In addition, as a brief exploration of the model's ability to extrapolate degradation beyond the measured data, the EKF was propagated forwards to a 10% increase in t^*, shown in slice (a) in Fig. 4. The extrapolation in this short range already shows divergence from the ground truth. The difference in the two extrapolations illustrates the limitations in capability of Gaussian processes to forecast out of the observed range. The ground truth function (26) is polynomial with respect to SoC, making it easier for the GP to extrapolate. In contrast, the sigmoid shape with respect to degradation limits the scope for GP extrapolation in this case. However, the performance in short-range extrapolation is arguably better than models that do not include any dynamics associated with the evolution of the parameters [9, 10, 12].

CONCLUSIONS

In order to enable stable and accurate battery state of health estimation and improve the usability of electrical equivalent circuit models in battery management systems with limited computational resources, a framework for functional parameter estimation was proposed. In this case resistance as a function of SoC and degradation was estimated by modelling it as a Gaussian process over two input dimensions. Using an extended Kalman filter, the posterior distribution of the function may be inferred recursively, with light computational load. The GP approximates the ground-truth of the functional parameter accurately, and can extrapolate across the SoC dimension in the case where the full SoC range is not observed.

The hyperparameters controlling the Gaussian process may also be estimated using a combination of the Kalman filter with Bayesian inference. This is computationally more intensive and thus should be done offline. A hybrid practical implementation might then consist of online functional estimation using hyperparameters calculated from large datasets e.g. in the cloud. The method may also be extended to estimate parameters in dynamic equations e.g. 1(b). However, this is more challenging - the joint state-parameter estimation problem becomes non-linear, and the Kalman filter approach may not be stable. Additionally, this method can be applied to estimate functional parameters in efficient reduced-order physics-based Li-ion models, where it is known from experimental data that some parameters, namely the solid state diffusivities, depend strongly on state of charge and degradation.

REFERENCES

[1] Särkkä, S., Solin, A., and Hartikainen, J., 2013. "Spatiotemporal learning via infinite-dimensional bayesian filtering and smoothing: A look at gaussian process regres-

sion through kalman filtering". *IEEE Signal Processing Magazine,* ***30***(4), pp. 51–61.

[2] Doyle, M., Fuller, T. F., and Newman, J., 1993. "Modeling of Galvanostatic Charge and Discharge of the Lithium/Polymer/Insertion Cell". *Journal of The Electrochemical Society,* ***140***(6), 6, p. 1526.

[3] Fuller, T., Doyle, M., and Newman, J., 1994. "Simulation and Optimization of the Dual Lithium Ion Insertion Cell". *Journal of the Electrochemical Society,* ***141***(1), pp. 1–10.

[4] Jokar, A., Rajabloo, B., Désilets, M., and Lacroix, M., 2016. "Review of simplified Pseudo-two-Dimensional models of lithium-ion batteries". *Journal of Power Sources,* ***327***, pp. 44–55.

[5] Gomez, J., Nelson, R., Kalu, E. E., Weatherspoon, M. H., and Zheng, J. P., 2011. "Equivalent circuit model parameters of a high-power Li-ion battery: Thermal and state of charge effects". *Journal of Power Sources,* ***196***(10), 5, pp. 4826–4831.

[6] Remmlinger, J., Buchholz, M., Meiler, M., Bernreuter, P., and Dietmayer, K., 2011. "State-of-health monitoring of lithium-ion batteries in electric vehicles by on-board internal resistance estimation". *Journal of Power Sources,* ***196***(12), pp. 5325–5331.

[7] Birkl, C. R., Roberts, M. R., McTurk, E., Bruce, P. G., and Howey, D. A., 2017. "Degradation diagnostics for lithium ion cells". *Journal of Power Sources,* ***341***, 2, pp. 373–386.

[8] Hartikainen, J., and Särkkä, S., 2010. "Kalman filtering and smoothing solutions to temporal Gaussian process regression models". *Proceedings of the 2010 IEEE International Workshop on Machine Learning for Signal Processing, MLSP 2010*(Mlsp), pp. 379–384.

[9] Plett, G. L., 2004. "Extended Kalman filtering for battery management systems of LiPB-based HEV battery packs: Part 3. State and parameter estimation". *Journal of Power Sources,* ***134***(2), 8, pp. 277–292.

[10] Plett, G. L., 2006. "Sigma-point Kalman filtering for battery management systems of LiPB-based HEV battery packs Part 2: Simultaneous state and parameter estimation". *Journal of Power Sources,* ***161***, pp. 1369–1384.

[11] Kim, J., Lee, S., and Cho, B. H., 2012. "Complementary cooperation algorithm based on DEKF combined with pattern recognition for SOC/capacity estimation and SOH prediction". *IEEE Transactions on Power Electronics,* ***27***(1), pp. 436–451.

[12] Baba, A., and Adachi, S., 2015. "Simultaneous state of charge and parameter estimation of lithium-ion battery using log-normalized unscented Kalman Filter". In 2015 American Control Conference (ACC), IEEE, pp. 311–316.

[13] Du, J., Liu, Z., Wang, Y., and Wen, C., 2016. "An adaptive sliding mode observer for lithium-ion battery state of charge and state of health estimation in electric vehicles". *Control Engineering Practice,* ***54***, 9, pp. 81–90.

[14] Kim, I. S., 2010. "A technique for estimating the state of health of lithium batteries through a dual-sliding-mode observer". *IEEE Transactions on Power Electronics,* ***25***(4), pp. 1013–1022.

[15] Bizeray, A. M., Kim, J. H., Duncan, S. R., and Howey, D. A., 2018. "Identifiability and Parameter Estimation of the Single Particle Lithium-Ion Battery Model". *IEEE Transactions on Control Systems Technology,* ***27***(5), pp. 1862–1877.

[16] Barai, A., Uddin, K., Widanalage, W. D., McGordon, A., and Jennings, P., 2016. "The effect of average cycling current on total energy of lithium-ion batteries for electric vehicles". *Journal of Power Sources,* ***303***, pp. 81–85.

[17] Reniers, J. M., Mulder, G., and Howey, D. A., 2019. "Review and Performance Comparison of Mechanical-Chemical Degradation Models for Lithium-Ion Batteries". *Journal of The Electrochemical Society,* ***166***(14), pp. A3189–A3200.

[18] Schimpe, M., von Kuepach, M. E., Naumann, M., Hesse, H. C., Smith, K., and Jossen, A., 2018. "Comprehensive Modeling of Temperature-Dependent Degradation Mechanisms in Lithium Iron Phosphate Batteries". *Journal of The Electrochemical Society,* ***165***(2), 1, pp. A181–A193.

[19] Rasmussen, C. E., and Williams, C. K. I., 2006. *Gaussian processes for machine learning*. Adaptive computation and machine learning. MIT, Cambridge, Mass. ; London.

[20] Lindgren, F., and Rue, H., 2011. "An explicit link between Gaussian fields and Gaussian Markov random fields: the stochastic partial differential equation approach". *Journal of the Royal Statistical Society. Series B,* ***73***(4), pp. 423–498.

[21] Murphy, K. P., 2012. *Machine learning : a probabilistic perspective*. Adaptive computation and machine learning. MIT Press, Cambridge, Mass.

[22] Quiñonero-Candela, J., and Rasmussen, C. E., 2005. "A unifying view of sparse approximate Gaussian process regression". *Journal of Machine Learning Research,* ***6***, pp. 1939–1959.

[23] Saatci, Y., 2011. "Scalable inference for structured Gaussian process models". *Dissertation*.

[24] Cressie, N., and Huang, H. C., 1999. "Classes of Nonseparable, Spatio-Temporal Stationary Covariance Functions". *Journal of the American Statistical Association,* ***94***(448), pp. 1330–1339.

[25] Särkkä, S., and Hartikainen, J., 2012. "Infinite-dimensional kalman filtering approach to spatio-temporal Gaussian process regression". *Journal of Machine Learning Research,* ***22***, pp. 993–1001.

[26] Davison, E. J., and Man, F. T., 1968. "The numerical solution of A'Q+QA = -C". *IEEE Transactions on Automatic Control,* ***13(4)***(August), p. 448–449.

[27] Hu, X., Li, S., Peng, H., and Sun, F., 2012. "Robust-

ness analysis of State-of-Charge estimation methods for two types of Li-ion batteries". *Journal of Power Sources,* ***217***, pp. 209–219.

[28] Gilks, W. R., Richardson, S., and Spiegelhalter, D. J., 1996. Markov chain Monte Carlo in practice.

[29] Kucukelbir, A., Blei, D. M., Gelman, A., Ranganath, R., and Tran, D., 2017. "Automatic Differentiation Variational Inference". *Journal of Machine Learning Research,* ***18***, pp. 1–45.

[30] Rauch, H. E., Tung, F., and Striebel, C. T., 1965. "Maximum likelihood estimates of linear dynamic systems". *AIAA Journal,* ***3***(8), pp. 1445–1450.

[31] Särkkä, S., 2013. *Bayesian Filtering and Smoothing*. Cambridge University Press.

[32] Gregory L. Plett, 2015. *Battery Management Systems, Volume II: Equivalent-Circuit Methods*. Artech House Publishers.

[33] D'Errico, J., 2020. "Adaptive robust numerical differentiation". *MATLAB Central File Exchange*(Retrieved March 30, 2020).